Biosensors and Bioelectronics 26 (2010) 841–845

Contents lists available at ScienceDirect

Biosensors and Bioelectronics

journal homepage: www.elsevier.com/locate/bios

Carbon electrodes for direct electron transfer type laccase cathodes investigated by current density–cathode potential behavior

Stefanie Rubenwolf[a], Oliver Strohmeier[a], Arne Kloke[a], Sven Kerzenmacher[a,*], Roland Zengerle[a,b], Felix von Stetten[a]

[a] Laboratory for MEMS Applications, Department of Microsystems Engineering-IMTEK, University of Freiburg, Georges-Koehler-Allee 103, 79110 Freiburg, Germany
[b] Centre for Biological Signalling Studies (bioss), Albert-Ludwigs-Universität Freiburg, Germany

ARTICLE INFO

Article history:
Received 23 September 2009
Received in revised form 16 February 2010
Accepted 4 May 2010
Available online 11 May 2010

Keywords:
Biofuel cell
Direct electron transfer
Carbon nanofibers
Carbon nanotubes
Graphite felt
Porous carbon tube

ABSTRACT

Direct electron transfer from carbon electrodes to adsorbed laccase (EC 1.10.3.2) from *Trametes versicolor* is widely used to enable mediatorless enzymatic biofuel cell cathodes. However, data published so far are poorly comparable in terms of oxygen reduction performance. We thus present a comparative characterization of carbon-based electrode materials as cathode in half-cell configuration, employing adsorbed laccase as oxygen reduction catalyst.

Open circuit potentials and performances were significantly increased by laccase adsorption, indicating the occurrence of direct electron transfer. At a potential of 0.5 V vs. SCE volume-normalized current densities of approximately 10, 37, 40, 70, and 77 $\mu A\,cm^{-3}$ were measured for cathodes nanotubes, carbon nanofibers and multi-walled carbon nanotubes, respectively.

In addition, we could show that both, carbon nanotubes and porous carbon tubes exhibit dramatically lower current densities compared to graphite felt and carbon nanofibers when normalized to BET surface instead of electrode volume. Further work will be required to clarify whether this stems from material-dependent interaction of enzyme and electrode surface or constricted enzyme adsorption due to agglomeration of the nanotubes. In case of the latter, an improved dispersion of the nanotubes upon electrode fabrication may greatly enhance their performance.

1. Introduction

The enzyme laccase (EC 1.10.3.2, benzenediol:oxygen oxidoreductase) from the white rot fungus *Trametes versicolor* is an attractive biocatalyst for oxygen reduction in enzymatic biofuel cell cathodes (Brunel et al., 2007; Habrioux et al., 2007; Liu and Dong, 2007; Tarasevich et al., 1979; Vincent et al., 2005; Yan et al., 2006). Both, laccase's capability to catalyze the four-electron reduction of dioxygen directly to water (Yaropolov et al., 1994) as well as the high redox potential of 0.820 V vs. SHE (0.579 V vs. SCE) (Solomon et al., 1996) promise biofuel cells with high power output, while as a glycosylated exoenzyme it is quite stable compared to other enzymes (Solomon et al., 1996). Furthermore, laccase supports the direct electron transfer with carbon-based electrode materials, onto which it is readily adsorbed (Kamitaka et al., 2007; Shleev et al., 2005; Vincent et al., 2005; Yan et al., 2006). This eliminates the need for redox polymers to electrically 'wire' the enzyme to an electrode, these being the main reason for fast performance loss of enzymatic biofuel cells in complex biological fluids (Binyamin et al., 2001).

For the construction of optimized biofuel cells with mediatorless laccase cathodes, the choice of electrode material is of prime interest. The oxygen reduction performance of carbon-adsorbed laccase under biofuel cell operating conditions can be compared based on the current density–cathode potential behavior at quasi-stationary conditions. But despite extensive literature, it is difficult to evaluate the influence of electrode material from published data. One reason is that in literature laccase cathodes are often investigated as complete fuel cells, together with a wide variety of enzymatically (Brunel et al., 2007; Heller, 2004; Kamitaka et al., 2007; Liu and Dong, 2007; Mano et al., 2003; Vincent et al., 2005; Yan et al., 2006) and abiotically catalyzed (Habrioux et al., 2007; Palmore and Kim, 1999) anodes, using glucose, fructose or hydrogen as fuel. If only overall cell voltage is measured rather than individual electrode potentials against a reference electrode (Liu

* Corresponding author at: Laboratory for MEMS Applications, Department of Microsystems Engineering-IMTEK, University of Freiburg, Georges-Koehler-Allee 103, 79110 Freiburg, Germany. Tel.: +49 761 203 7328; fax: +49 761 203 7322.
E-mail addresses: stefanie.rubenwolf@imtek.uni-freiburg.de (S. Rubenwolf), oliver.strohmeier@imtek.uni-freiburg.de (O. Strohmeier), arne.kloke@imtek.uni-freiburg.de (A. Kloke), kerzenma@imtek.uni-freiburg.de (S. Kerzenmacher), zengerle@imtek.uni-freiburg.de (R. Zengerle), vstetten@imtek.uni-freiburg.de (F. von Stetten).

0956-5663/$ – see front matter © 2010 Elsevier B.V. All rights reserved.
doi:10.1016/j.bios.2010.05.008

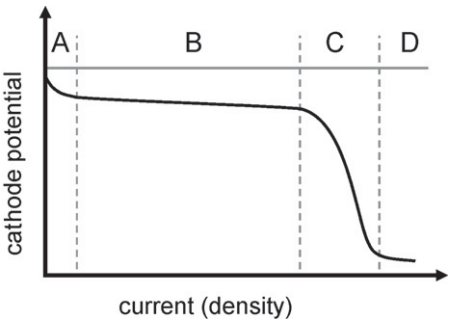

Fig. 1. Typical current (density)–potential behavior of a biofuel cell cathode. The thermodynamic reversible half-cell potential is indicated by a gray line and differs from the actually reached cathode potential at open circuit conditions. With increasing current (density) the cathode potential decreases, in four steps: (A) potential drop due to activation overpotential, (B) linear potential losses due to ohmic resistances, (C) potential drop due to mass transport limitations, (D) potential stabilization caused by further reactions (Larminie and Dicks, 2000).

and Dong, 2007; Vincent et al., 2005; Yan et al., 2006), the polarization behavior of anode and cathode cannot be evaluated separately. But only independent characterization of individual electrodes can help identifying the reasons for irreversible potential losses and thereby show the bottlenecks of fuel cell performance. Furthermore, most experimental setups do not feature a membrane to separate anode and cathode compartment (Brunel et al., 2007; Habrioux et al., 2007; Kamitaka et al., 2007; Liu and Dong, 2007; Mano et al., 2003; Shleev et al., 2005; Vincent et al., 2005; Yan et al., 2006). Cross-talk by substrates and products from the anode reaction can thus not be excluded.

In the present work we therefore use a two-compartment setup to investigate mediatorless laccase cathodes as half-cell electrodes under galvanostatic load, independently of the counter electrode. The quasi-stationary current density–cathode potential behavior is used to systematically characterize the oxygen reduction performance of cathodes with different electrode materials. Under investigation are carbon-based electrode materials that are of potential interest for the use in miniaturized enzymatic biofuel cells. Since in the micro-domain volume often dominates over weight or geometric area, the concept of volume-normalized current density is used to evaluate the current density–cathode potential behavior of the individual electrode materials.

1.1. Current (density)–cathode potential behavior in enzymatically catalyzed biofuel cells

In Fig. 1 the typical current density–potential behavior of an enzymatically catalyzed biofuel cell cathode is shown. Even at open circuit conditions the electrode potential is lower than its reversible half-cell potential due to redox potentials of enzyme or mediator (Barton et al., 2004) and surrounding conditions as temperature or reactant concentrations (Larminie and Dicks, 2000). When current is applied, there are further irreversible potential losses:

(A) Activation losses cause a first potential drop at low current densities, due to slowness of the chemical reaction consuming electrons from the electrode. They can be reduced by increasing temperature, roughness of the electrode or enzyme loading (Larminie and Dicks, 2000).
(B) A slower and fairly linear potential decay is caused by ohmic resistances in electrode, electric circuit and electrolyte (Hamnett, 2003; Larminie and Dicks, 2000). Also the tunneling resistance in direct electron transfer exhibits ohmic behavior at low current densities, before decreasing with increasing current density (Knauss and Breslow, 1962; Simmons, 1963).
(C) Concentration limitations due to insufficient mass transport result in a considerable potential drop (Larminie and Dicks, 2000). Substrate concentration at the electrode surface can be decreased by limited diffusion within porous electrodes as well as insufficient substrate intake e.g. when gassing with air to supply oxygen (Hamnett, 2003). Other limiting factors can be diffusion of protons or mediator (Kim et al., 2006). Catalytic activity (Tsujimura, 2007) can on the one hand be limited by reaction velocity, given by the turn-over number of the enzymes and surrounding conditions. On the other hand it can be limited by the number of involved enzymes, influenced by enzyme inactivation and in case of direct electron transfer also enzyme adsorption and orientation.
(D) The electrode potential can stabilize again when a second reaction such as electrolysis occurs.

2. Materials and methods

2.1. Chemicals and electrode materials

Laccase from *T. versicolor*, sodium hydrogencitrate sesquihydrate, sodium dihydrogencitrate, and 2,2′-azino-bis(3-ethylbenzothiazoline-6-sulfonic acid) diammonium salt (ABTS) were purchased from Sigma–Aldrich (Taufkirchen, Germany). α-D(+)-Glucose monohydrate and 2-propanol were supplied by Carl Roth (Karlsruhe, Germany). Aqueous solutions were prepared using deionized water. As electrode materials both, solid three-dimensional materials (graphite felt and porous carbon tubes) as well as powdery nanomaterials (carbon nanofibers and carbon nanotubes) were investigated as summarized in Table 1. All chemicals and electrode materials were used as received.

Table 1
Tested electrode materials. The volume specific surface area of powdery nanomaterials and porous carbon tubes was determined by the one-point BET method. Densities of nanomaterials are measured bulk densities of the dry material. All other data provided by the suppliers.

Three-dimensional material	Dimensions	Surface area ($m^2\,cm^{-3}$)	Density ($g\,cm^{-3}$)	Supplier
(a) Graphite felt	Fiber diameter ~2 μm Fiber length >5 cm	0.059	0.082	Alfa Aesar (Karlsruhe, Germany)
(b) Porous carbon tube	Outer diameter 10 mm Inner diameter 6 mm 25% porosity	2.6	1.7	Novasep (Epone, France)

Powdery nanomaterial	Length (μm)	Diameter (nm)	Surface area ($m^2\,cm^{-3}$)	Density ($g\,cm^{-3}$)	Supplier
(c) Carbon nanofibers (HTF150FF LHT)	>20	100–200	0.54	0.044	Electrovac (Klosterneuenburg, Austria)
(d) Multi-walled carbon nanotubes (MT MW 000 010)	5–15	<10	7.8	0.045	Carbon NT&F 21 Zoettl (Eisenstadt, Austria)
(e) Single-walled carbon nanotubes (MT SW HPO 002)	<20	<2	17	0.045	Carbon NT&F 21 Zoettl (Eisenstadt, Austria)

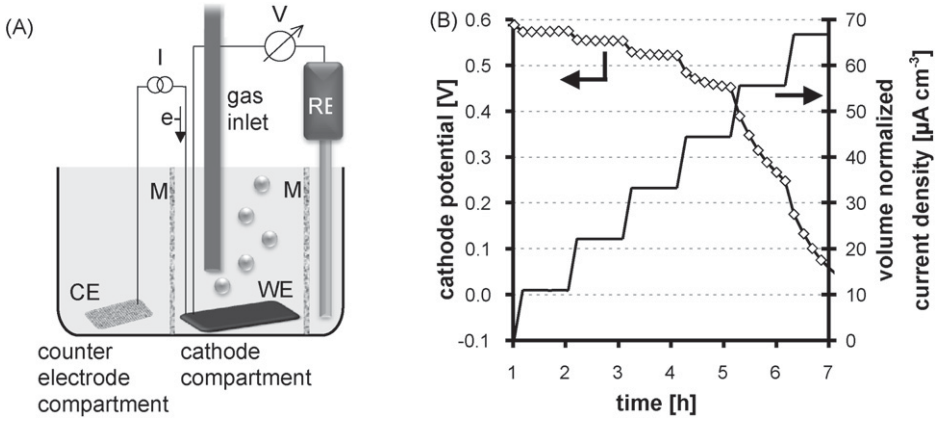

Fig. 2. Electrochemical characterization of cathodes. (A) Test setup for the evaluation of cathodes. Working electrode (WE), platinum mesh as counter electrode (CE) and a saturated calomel electrode as reference electrode (RE) are in compartments separated by Fumion®-membranes (M). The cathode compartment is bubbled with air. Current is applied by an electronic load (*I*), cathode potential (*V*) is measured against the reference electrode. (B) Time-dependent progression of the cathode potential, when the current is increased stepwise every hour to record the current density–cathode potential behavior, exemplary shown for a porous carbon tube electrode.

The real surface areas of the electrode materials were determined by the one-point BET method from nitrogen adsorption isotherms (30% nitrogen and 70% helium, Flow Sorb 2300 and De Sorb 2300, Micromeritics, Mönchengladbach, Germany).

2.2. Preparation of electrodes

While solid materials were cut into pieces not larger than 1 cm^3, the powdery nanomaterials were immobilized by clamping them between two sheets of permeable membranes, together with platinum mesh (Goodfellow, Huntingdon, UK) as current collector. Hereto paper tissue (Kimtech from Kimberly-Clark, Reigate, UK) was used in case of carbon nanofibers, whereas the smaller diameter carbon nanotubes demanded cellulose acetate filters with a pore size of 0.45 μm (Sartorius, Göttingen, Germany). To eliminate the influence of contact resistances two separate platinum wires (0.1 mm diameter/99.9%, Chempur, Karlsruhe, Germany) for electrode current and voltage were used, attached to the electrode with conductive carbon cement (Leit-C, Plano, Wetzlar, Germany). Prior to assembly in the test cell, the electrodes were wetted with 2-propanol, washed thoroughly with deionized water, and transferred into 0.1 M citrate buffer at pH 5.

2.3. Electrochemical test cell and measurement setup

The electrochemical test cell used in this work is already described in detail elsewhere (Kloke et al., 2010). As shown schematically in Fig. 2A, it consists of two polycarbonate compartments, separated by a proton permeable Fumion®-membrane (FuMA-Tech, St. Ingbert, Germany) to prevent electrode cross-talk by substrates or reaction products. In the present work the cathode compartment was continuously bubbled with humidified air to saturate the electrolyte with oxygen. A saturated calomel electrode (SCE, Sensortechnik, Meinsberg, Germany) was used as reference electrode, plain platinum mesh served as counter electrode.

The electrical setup for recording current density–cathode potential curves is described elsewhere (Kerzenmacher et al., 2009). In short, it consists of an electronic load (STG 2008 stimulus generator, Multichannel Systems, Reutlingen, Germany), enabling galvanostatic operation of the cathode against an arbitrary counter electrode. With our setup the possible current range is thus no longer limited by the performance of the counter electrodes (anodes), in contrast to other approaches with passive load resistors (Kamitaka et al., 2007; Liu and Dong, 2007; Palmore and Kim, 1999; Vincent et al., 2005). A computer-controlled Keithley 2700 integrated multimeter/data acquisition system (Keithley, Germering, Germany) is used to record the cathode potential against the saturated calomel reference electrode in intervals of 10 min.

2.4. Test protocol

Prior to testing, the electrochemical two-chamber cells were equipped with electrodes, filled with 0.1 M citrate buffer pH 5, and autoclaved to remove bubbles in the liquid channel interconnecting the compartments of cathode and counter electrode. Subsequently, the buffer in the counter electrode compartment was exchanged against 4 ml citrate buffer with additionally 1 g L^{-1} glucose. Depending on the type of experiment, the testing solution in the cathode compartment was exchanged as described in the following.

To investigate the inherent oxygen reduction performance of the electrode material in the absence of laccase 4 ml of fresh citrate buffer were used in the cathode compartment.

The direct electron transfer between adsorbed laccase and the electrode material in the absence of a mediator was investigated by using 4 ml citrate buffer, additionally containing 20 U laccase.

To record comparable current density–cathode potential curves under conditions of mediated electron transfer, only enzyme previously adsorbed to the electrode should be involved in the reaction. Thereto 20 U laccase in citrate buffer was allowed to adsorb on the electrode for at least 1.5 h. Subsequently the testing solution was exchanged against laccase-free citrate buffer containing 0.02 M ABTS as mediator.

After stabilization of the cathode open circuit potential (potential drift < 5 mV h^{-1}) the load current was increased from 0 μA to 100 μA in steps of 5 μA per hour to record current density–cathode potential curves (shown exemplarily in Fig. 2B). All experiments were performed at room temperature. To exclude the possible influence of electrode history on performance, always freshly prepared electrodes were used. Similarly, each type of experiment was repeated at least three times with freshly prepared electrodes.

2.5. Data analysis and presentation

Fig. 2B shows a representative time-dependent progression of cathode potential when the current is increased in hourly steps of 5 μA. As can be seen, for potentials above 0.5 V the electrode potential reaches stable values within 1 h time interval. This is the case for all materials investigated within this work, where at

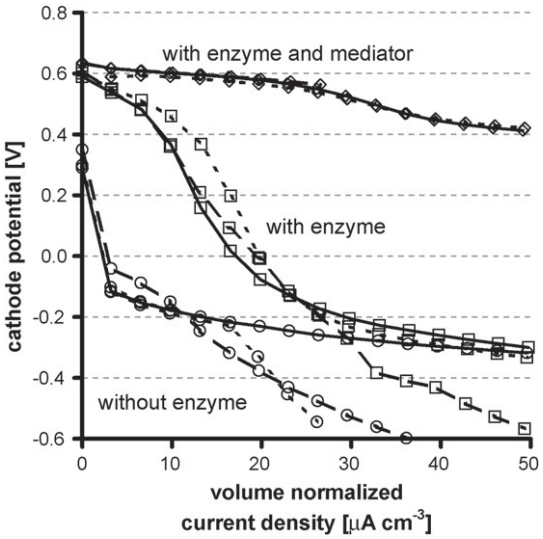

Fig. 3. Comparison of direct and mediated electron transfer, shown exemplarily for graphite felt electrodes. Each three electrodes were characterized without addition of laccase, with addition of laccase and ABTS as mediator.

electrode potentials around 0.5 V and above potential drifts of typically <5 mV h^{-1} and at maximum 17 mV h^{-1} are displayed. To obtain representative values for quantitative analysis we therefore chose to compare the electrode current density exhibited at a cathode potential of 0.5 V.

Current density–cathode potential curves were constructed from the cathode potentials recorded vs. the reference electrode after 1 h of operation at a given current density. The current density was normalized either to the volume of the electrode material under investigation, calculated from weight and bulk density of the dry electrode material, or it was normalized to the BET surface area (see Table 1). Bars in graphs represent the minimum and maximum value of three separate experiments.

3. Results and discussion

3.1. Identification of performance limiting factors

In the absence of laccase all investigated materials exhibit an open circuit potential between 0.2 V and 0.4 V vs. SCE due to the inherent catalytic activity of carbon towards oxygen reduction (Kerzenmacher et al., 2008; Kim et al., 2004; Stigter et al., 1997; Yeager, 1984). Addition of laccase to the testing solution greatly shifts the electrode open circuit potential towards more positive values in the range of 0.6 V vs. SCE, and also significantly improves the oxygen reduction performance of all tested materials as shown exemplarily for graphite felt in Fig. 3. This clearly shows that laccase activity dominates electrode performance and indicates the occurrence of direct electron transfer between the enzyme and the carbon-based electrode materials. With increasing current density all cathodes show the distinctive drop in electrode potential commonly attributed to the occurrence of mass-transfer limitations as described in Section 2. However, in the experiments with adsorbed enzyme and the mediator ABTS in the testing solution all electrode materials showed a significantly improved performance with mass-transfer limitations occurring at higher current densities as shown exemplarily for graphite felt in Fig. 3. This indicates that the sudden potential drop does not result from a setup inherent limitation as oxygen intake or proton diffusion within the ion bridge. Rather are the observed transport limitations associated with the electrode material as for instance oxygen diffusion within porous electrodes, enzyme adsorption or its orientation at the electrode surface.

3.2. Direct comparison of electrode materials in terms of electrode volume

In Fig. 4A the volume-normalized current density–potential plots of different materials with adsorbed laccase as oxygen reduction catalyst are compared. As can be seen, electrodes fabricated from graphite felt show a distinctively low performance, the volume-normalized current density at 0.5 V vs. SCE amounting to <10 μA cm^{-3}. At the same electrode potential, approximately 37 μA cm^{-3} can be sustained with electrodes from porous carbon tubes, and approximately 40 μA cm^{-3} with those from single-walled carbon nanotubes. Among the investigated materials, electrodes from carbon nanofibers and multi-walled carbon nanotubes exhibit the highest performance, their volume-normalized current densities at 0.5 V vs. SCE amounting to approximately 70 and 77 μA cm^{-3}, respectively.

3.3. Direct comparison of electrode materials in terms of electrode surface area

As shown in Table 1, electrodes of the same geometric area can differ greatly in their real surface area when fabricated from the different materials. It is therefore also of interest to relate the electrode performance to the real surface area of the materials. This comparison is shown in Fig. 4B, where the cathode potential is plotted against the current density normalized to the BET

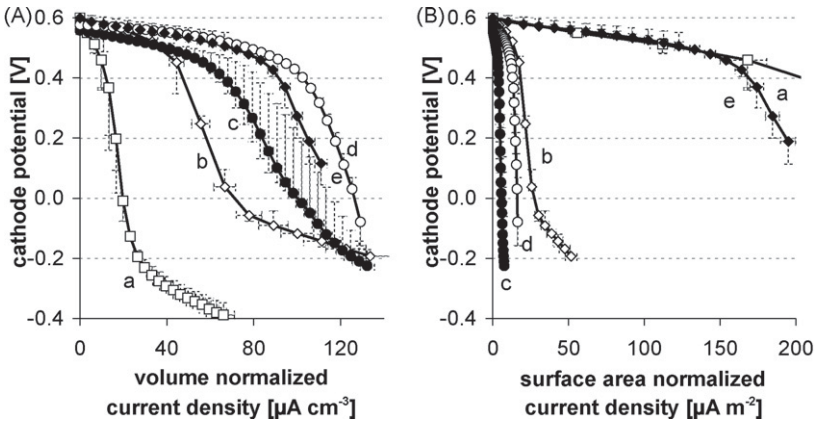

Fig. 4. Current density–cathode potential plots for the electrodes with laccase adsorbed to the following materials: graphite felt (a), porous carbon tubes (b), single-walled carbon nanotubes (c), multi-walled carbon nanotubes (d), and carbon nanofibers (e). (A) Comparison of cathode performance with a current density normalized to volume. (B) Comparison of cathode performance with a current density normalized to BET surface area.

surface area of the electrodes. At 0.5 V vs. SCE the electrodes from graphite felt and carbon nanofibers exhibit similar current densities of approximately 125 and 129 $\mu A\,m^{-2}$, respectively. The fact that carbon nanofiber electrodes show a better volume-normalized performance than graphite felt electrodes (Fig. 4A) can thus be clearly related to the higher real surface area per volume.

Remarkably, the current densities of electrodes from porous carbon tubes and multi-walled carbon nanotubes at 0.5 V vs. SCE are nearly one order of magnitude lower than those from graphite felt and carbon nanofibers, amounting to approximately 14 and 10 $\mu A\,m^{-2}$, respectively. Furthermore, with only approximately 2 $\mu A\,m^{-2}$ single-walled carbon nanotube electrodes exhibit the lowest current density at 0.5 V vs. SCE when normalized to BET surface area. These results suggest that with both, the investigated carbon nanotubes and the porous carbon tubes not all of the surface area is involved in the electrochemical reaction. This may be due to material-dependent interaction of enzyme and electrode surface, or limited enzyme adsorption to the materials. In case of the porous carbon tubes, the latter hypothesis may be explained by small pores and long diffusion paths. Similarly, the small diameter nanotubes may form aggregates and thus reduce the surface availability for enzyme adsorption.

4. Conclusions

To our best knowledge, the present work is the first attempt to investigate the influence of electrode material on the performance of mediatorless biofuel cell cathodes with adsorbed laccase as oxygen reduction catalyst. Thereto graphite felt, porous carbon tubes, carbon nanofibers as well as single-walled and multi-walled carbon nanotubes were characterized as half-cell electrodes under comparable experimental conditions using current density–cathode potential plots.

For all the investigated materials open circuit potential and performance was significantly increased by laccase adsorption, indicating the occurrence of direct electron transfer. The comparison of electrode performance under conditions of direct and also mediated electron transfer showed, that the lower performance encountered in the absence of the mediator is not due to a setup inherent limitation but rather electrode material depended parameters as oxygen diffusion within porous electrodes, enzyme adsorption or its orientation at the electrode surface

In terms of volume-normalized current density, multi-walled carbon nanotubes showed the best performance among the investigated materials, exhibiting approximately 77 $\mu A\,cm^{-3}$ at 0.5 V vs. SCE. However, the results also revealed that carbon nanotubes and porous carbon tubes exhibit dramatically lower current densities at 0.5 V vs. SCE when normalized to BET surface area. Further work will be required to clarify whether this stems from a material-dependent rate of direct electron transfer or constricted enzyme adsorption due to agglomeration of the nanotubes. In case of the latter, an improved dispersion of the nanotubes upon electrode fabrication may greatly enhance their performance.

Acknowledgements

Financial support by the German Research Association (DFG) through the PhD program “Micro Energy Harvesting” (GRK 1322) and the German Ministry of Education and Research (BMBF) under the program Bioenergie2021 (Grant No. 03SF0382) is gratefully acknowledged. The authors thank Margarethe Offermann from the Forschungszentrum Karlsruhe for doing the BET measurements. Porous carbon tubes were a gift from Novasep, and multi-walled carbon nanotubes were a gift from Carsten Glanz, Fraunhofer TEG, Stuttgart.

References

Barton, S.C., Gallaway, J., Atanassov, P., 2004. Chem. Rev. 104 (10), 4867–4886.
Binyamin, G., Chen, T., Heller, A., 2001. J. Electroanal. Chem. 500 (1–2), 604–611.
Brunel, L., Denele, J., Servat, K., Kokoh, K.B., Jolivalt, C., Innocent, C., Cretin, M., Rolland, M., Tingry, S., 2007. Electrochem. Commun. 9 (2), 331–336.
Habrioux, A., Sibert, E., Servat, K., Vogel, W., Kokoh, K.B., Alonso-Vante, N., 2007. J. Phys. Chem. B 111 (34), 10329–10333.
Hamnett, A., 2003. In: Vielstich, W., Lamm, A., Gasteiger, H. (Eds.), Handbook of Fuel Cells – Fundamentals, Technology, Applications. John Wiley & Sons, Ltd., Chichester, England, pp. 3–12.
Heller, A., 2004. Phys. Chem. Chem. Phys. 6 (2), 209–216.
Kamitaka, Y., Tsujimura, S., Setoyama, N., Kajino, T., Kano, K., 2007. Phys. Chem. Chem. Phys. 9 (15), 1793–1801.
Kerzenmacher, S., Ducrée, J., Zengerle, R., von Stetten, F., 2008. J. Power Sources 182 (1), 66–75.
Kerzenmacher, S., Mutschler, K., Kräling, U., Baumer, H., Ducrée, J., Zengerle, R., von Stetten, F., 2009. J. Appl. Electrochem. 39 (9), 1477–1485.
Kim, B.H., Park, H.S., Kim, H.J., Kim, G.T., Chang, I.S., Lee, J., Phung, N.T., 2004. Appl. Microbiol. Biotechnol. 63 (6), 672–681.
Kim, J., Jia, H.F., Wang, P., 2006. Biotechnol. Adv. 24 (3), 296–308.
Kloke, A., Rubenwolf, S., Bücking, C., Gescher, J., Kerzenmacher, S., Zengerle, R., von Stetten, F., 2010. Biosens. Bioelectron, doi:10.1016/j.bios.2010.04.014.
Knauss, H.P., Breslow, R.A., 1962. Proc. Inst. Radio Eng. 50 (8), 1834.
Larminie, J., Dicks, A., 2000. Fuel cell systems explained. John Wiley & Sons, Ltd., Chichester, England.
Liu, Y., Dong, S., 2007. Biosens. Bioelectron. 23 (4), 593–597.
Mano, N., Mao, F., Shin, W., Chen, T., Heller, A., 2003. Chem. Commun. (4), 518–519.
Palmore, G.T.R., Kim, H.H., 1999. J. Electroanal. Chem. 464 (1), 110–117.
Shleev, S., Jarosz-Wilkolazka, A., Khalunina, A., Morozova, O., Yaropolov, A., Ruzgas, T., Gorton, L., 2005. Bioelectrochemistry 67 (1), 115–124.
Simmons, J.G., 1963. J. Appl. Phys. 34 (1), 238–239.
Solomon, E.I., Sundaram, U.M., Machonkin, T.E., 1996. Chem. Rev. 96 (7), 2563–2605.
Stigter, E.C.A., Dejong, G.A.H., Jongejan, J.A., Duine, H.A., Vanderlugt, J.P., Somers, W.A.C., 1997. J. Chem. Technol. Biotechnol. 68 (1), 110–116.
Tarasevich, M.R., Yaropolov, A.I., Bogdanovskaya, V.A., Varfolomeev, S.D., 1979. Bioelectrochem. Bioeng. 6 (3), 393–403.
Tsujimura, S., 2007. Studies on Energy Conversion Systems Based on Bioelectrocatalytic Reactions. Kyoto University Research Information Repository.
Vincent, K.A., Cracknell, J.A., Lenz, O., Zebger, I., Friedrich, B., Armstrong, F.A., 2005. Proc. Natl. Acad. Sci. U.S.A. 102 (47), 16951–16954.
Yan, Y.M., Zheng, W., Su, L., Mao, L.Q., 2006. Adv. Mater. 18 (19), 2639–2643.
Yaropolov, A.I., Skorobogatko, O.V., Vartanov, S.S., Varfolomeyev, S.D., 1994. Appl. Biochem. Biotechnol. 49 (3), 257–280.
Yeager, E., 1984. Electrochim. Acta 29 (11), 1527–1537.